THEORY OF FLOW IN THE CONDUCTIVITY PROBLEM OF INHOMOGENEOUS MEDIA

G. N. Dul'nev and V. I. Malarev

UDC 537.11.33

Based on flow theory, we provide the basis of the geometric structure of inhomogeneous materials, including phase transitions, and we suggest methods of calculating the conductivity of these systems.

1. Geometry of Clusters and Conductivity of Inhomogeneous Media. Problems related to flow theory were first formulated by Broadbent and Hammersley [1], based on which was created the mathematical discipline called flow theory. It has been widely used in various areas of physics, particularly in investigating the conductivity of inhomogeneous media. The flow problem and its application in the study of conductivity of inhomogeneous media are available in a substantial number of reviews [2-9]; therefore, in the present study we mostly consider problems related to the geometric interpretation of percolation effects in transport processes.

Imagine that in Fig. 1a the whole planar space is filled with isolating particles (white particles), later randomly impregnated by conductors (black particles). As shown by computer Monte Carlo calculations, at low concentrations m_M (M denotes the metal) of the conducting component the conducting regions are manifested singly or in the form of clusters (Fig. 1b, c), forming isolated clusters (IC) in this case. When the concentration increases and becomes equal to a critical m_c, an infinite cluster (IFC) is generated in the system, extending over all space, and the system becomes conducting; in Fig. 1c the dashed lines mark the flow paths through the IFC. For increasing $m_M > m_c$ the infinite cluster is enhanced, absorbing less clusters, and the conducting chains penetrate the whole system, forming a structure with mutually penetrating components. With further increase in m_M the isolating IFC disappears, while for $m_M = 1$ the whole space is filled by the conductor (Fig. 1e). The value $m_M = m_c$ is the so-called flow threshold, or the percolation threshold. In [2-4, 7] and in other studies it was shown that the existence of a percolation threshold is a general effect, inherent in both systems without a regular structure and in lattice models. Assuming that the conductivity of the isolating structure Λ equals 0, for $m_M < m_c$ the conductivity of the whole system must also be 0. At the threshold concentration value $m_M = m_c$ the system conductivity Λ undergoes a jump from zero to a finite value. The following expression is

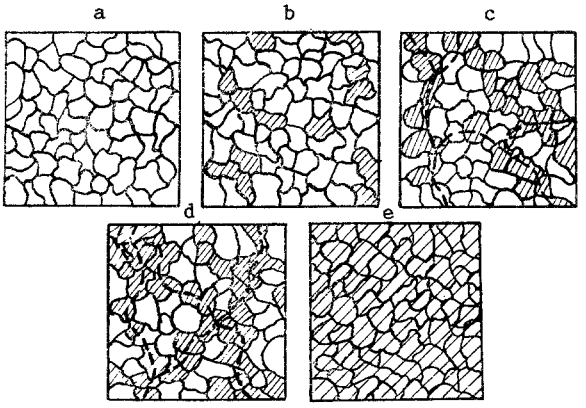

Fig. 1. Model of a binary inhomogenous body: a) $m_M = 0$; b) $m_M < m_c$; c) $m_M = m_c$; d) $m_M > m_c$; e) $m_M = 1$.

Leningrad Institute of Mechanics and Optics. Translated from Inzhenerno-Fizicheskii Zhurnal, Vol. 59, No. 3, pp. 522-539, September, 1990. Original article submitted January 23, 1990.

0022-0841/90/5903-1217$12.50

assumed within flow theory for the effective conductivity of the spatial two-component extremely inhomogeneous ($\Lambda_i/\Lambda_M = 0$) system for $m_M > m_c$ near the percolation threshold [3, 10]:

$$\frac{\Lambda}{\Lambda_M} = A(m_M - m_c)^k, \quad m_c = 0.15 \pm 0.03; \quad k = 1.8 \pm 0.2. \tag{1}$$

The values of A are less definite, and vary within the literature sources within the limits A = 1-1.6.

The theoretical results were generalized in [11, 12] to the cases $\Lambda_i/\Lambda_M \neq 0$ and $0 \leq m_M \leq 1$. The following dependences were recommended for the three concentration regions at $\Lambda_i/\Lambda_M = 5 \cdot 10^{-4}$:

$$\frac{\Lambda}{\Lambda_i} = (1 - 5m_M)^{-1} \text{ for } m_M < m_c; \tag{2}$$

$$\frac{\Lambda}{\Lambda_i} = 1.6(m_M - m_c)^{1.6} \text{ for } m_c \leqslant m_M < 0.5. \tag{3}$$

If $m_M > 0.5$, it is recommended to determine Λ from the following equation, obtained for an effective medium:

$$\frac{\Lambda}{\Lambda_M} = \frac{1}{4}((3m_M - 1) + (3m_i - 1)\nu) + \sqrt{\frac{\nu}{2} + \frac{1}{16}((3m_M - 1) + (3m_i - 1)\nu)^2}, \tag{4}$$

where $\nu = \Lambda_i/\Lambda_M$.

If $3 \cdot 10^{-2} \leq \nu < 1$, then Eq. (4) is recommended in the whole concentration region. Expression (4) was first obtained by Von Bruggemann in 1935 [13], then multiply rederived [14, 15], and is known in the literature as the Kondorskii–Odelevskii equation [16].

The diversity of equations, the formal nature of deriving them, and the absence of geometrically clear models provided incentives for searching new methods of solving the problem of effective conductivity. This conclusion is drawn by critical analysis of the equations describing the conductivity of sharply fixed structures of heterogeneous media (closed inclusions, mutually penetrable components), since they do not include the possibility of transition of one structure into another with a change in concentration, the appearance of jump conductivity at $m_M = m_c$ for extremely inhomogeneous media, and the statistical nature of component distribution in several systems.

Dul'nev and Novikov have suggested a method of constructing a flow theory and the reduction to an elementary unit cell [17]. In constructing the model they started from the established fact that for $\Lambda_i/\Lambda_M = 0$ the dependence $\Lambda = f(m_M)$ obeys the law (1). In this case, the concentration m_C of the conducting component, associated with the IFC, must obey the obvious conditions: $m_C = 0$ when the clusters are isolated, i.e., for values $m_M < m_c$; and $M_C = 1$ for total filling of the object by the conducting component. These conditions are satisfied by the dependence $m_C = (m_M - m_c)/(1 - m_c)$, $m_M \geq m_c$.

We note that the IFC concentration is measured here not from 0, but from the value of m_c, i.e., from the moment of IFC formation.

Assuming in expression (1) $A = (1 - m_c)^{-1.6}$, we represent the equation for Λ for extremely inhomogeneous systems ($\Lambda_i/\Lambda_M = 0$) in the form

$$\Lambda = \Lambda_M \left(\frac{m_M - m_c}{1 - m_c}\right)^{1.6}, \quad m_c \leqslant m_M \leqslant 1. \tag{5}$$

Equation (5) is definitely an approximation, but describes quite well the theoretical and experimental data (the error is less than 2% for k = 1.6).

A geometric model was constructed in [17, 18] of isolated and infinite clusters, reflecting the complex variation dynamics of the structure of an inhomogeneous system with the concentration of one of the components increasing from 0 to 1. For this purpose, heterogeneous systems of macroscopic cubes of edge L were separated in the volume, and the following restrictions were applied:

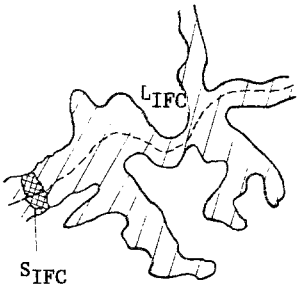

Fig. 2. Infinite cluster model.

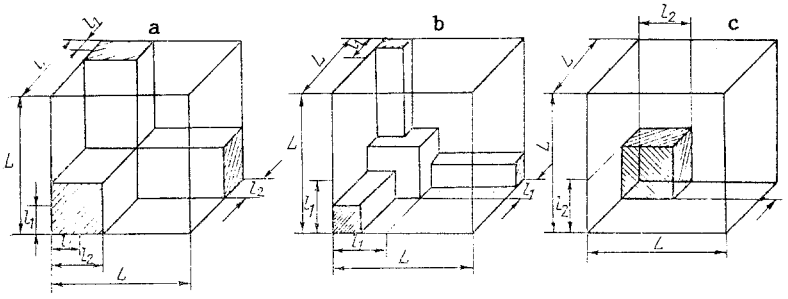

Fig. 3. Inhomogeneous system model: a) general shape of infinite cluster; b) system with mutually penetrable components; c) system with isolated inclusions.

L is the minimum distance for which the cube conductivity equals the effective conductivity Λ of the inhomogeneous system; in different words, the isolated element is representative;

the inhomogeneity sizes exceed the mean free path of the flux carriers (charge, energy, momentum, mass);

the cube resistance to the current $\langle j \rangle$ flowing along the normal to one of the sides equals $R = L/(\Lambda S)$, $S = L^2$.

The resistance R_{IFC} of the conducting IFC is, by definition, proportional to the mean length L_{IFC} of the current line, and is inversely proportional to the conductivity Λ_M of the infinite cluster and its averaged area of the transverse cross section S_{IFC} (Fig. 2), i.e., $R_{IFC} = L_{IFC}/(\Lambda_M S_{IFC})$. If $\Lambda_i/\Lambda_M = 0$, the resistances of the cube R and of IFC are equal, $R = R_{IFC}$ and

$$\Lambda = \Lambda_M \bar{S}_1, \quad \bar{S}_1 = \frac{S_{IFC} L}{S L_{IFC}}. \tag{6}$$

Comparing (5) and (6), we obtain the variation law of the effective transverse cross section $\bar{S}_1$ of the conducting IFC:

$$\bar{S}_1 = \left(\frac{m_M - m_c}{1 - m_c} \right)^{1.6}, \tag{7}$$

in which both the complex IFC topology and the probabilistic nature of its formation were taken into account.

We represent the IFC geometric shape in a cube of size L in the form illustrated in Fig. 3a. Here the ICs are modeled by separate cubic inclusions (of size ℓ_2) with concentration $m_M' = (\ell_2/L)^3$. The ICs are located at distances $\ell_3 = L - \ell_2$ from each other, and are joined by conducting couplers, whose transverse cross sections are ℓ_1^2.

The geometric structure of the model of an inhomogeneous binary structure varies in this representation with increasing concentration m_M: at low concentrations $m_M = m_M' < m_c$ there exist closed inclusions (IC) in the system, and with increasing m_M' they reach the limiting size $\ell_{2max} = L \sqrt[3]{m_c}$ (Fig. 3c). The first bridges between IC start appearing later on, with their transverse cross-section area and length being ℓ_1^2 and $(L - \ell_2)$. Further increase in the concentration m_M leads to an enhanced transverse cross-section area ℓ_1^2 of

the bridge until the ℓ_1 and ℓ_2 values are comparable, and the heterogeneous systems transform into a structure with mutually penetrating components (Fig. 3b). It is noted that all the complexity of the IFC geometry (its branching, nonuniformity of cross section, presence of internal voids, etc.) and the probabilistic nature of its formation process are concentrated in the present model in the effective transverse cross-section area and are represented by expression (7).

The mathematical model of the carrier transport process through the described structure of a binary mixture can be obtained by using the method of Rayleigh cross sections, whose justification and possible limitations are discussed in [19]. In this approach one uses the subdivision of an elementary unit cell by infinitely thin planes impenetrable to the flow (adiabatic subdivision). The more accurate method of combined subdivision is not given here only due to its awkwardness, but no major difficulties arise in this case. The equation for the effective conductivity of the heterogeneous system is

$$\frac{\Lambda}{\Lambda_M} = \bar{S}_1 + \nu\left(\frac{\Delta\bar{S}}{1-(1-\nu)\bar{l}_2} + \frac{2\bar{S}_3}{1-(1-\nu)\bar{l}_1} + \bar{S}_4\right), \tag{8}$$

where

$$\Delta\bar{S} = \bar{S}_2 - \bar{S}_1,\ \bar{l}_2 = m_c^{1/3},\ \text{if}\ \ \bar{S}_2 > \bar{S}_1,$$

$$\Delta\bar{S} = 0,\ \bar{l}_2 = \bar{l}_1,\ \text{if}\ \ \bar{S}_2 \leqslant \bar{S}_1;$$

$$\bar{S}_1 = \bar{l}_1^2,\ \bar{S}_2 = \bar{l}_2^2,\ \bar{S}_3 = (1-\bar{l}_2)\bar{l}_1,\ \bar{S}_4 = 1-\bar{S}_2-2\bar{S}_3,$$

$$\bar{l}_1 = \left(\frac{m_M - m_c}{1-m_c}\right)^{0.8},\ \nu = \Lambda_i/\Lambda_M.$$

The dependence (8) takes into account the variation of the heterogeneous system structure for the concentration m_M increasing from 0 to 1:

for $m_M = m_M' < m_c$ there exist only closed inclusions (IC) in the structure;

for $m_c \leq m_M \leq 0.5$, conducting bridges are generated between IC; their transverse cross-section area increases, and for $m_M = 0.5$ a structure occurs with mutually penetrating components;

for $0.5 \leq m_M \leq 1$, there is a uniform growth in component M, having a structure with mutually penetrating components. If it is also necessary to take into account the variation in IFC and IC geometries of the insulating components, in this case, following the generation of a structure with mutually penetrating components it is necessary to carry out an inversion of expression (8), i.e., the subscript M is replaced by i.

In the following we carry out a correction of the flow theory method as applied to an elementary unit cell, and a refinement of the equations of [20]. In this case the calculation accuracy is not increased substantially, while the calculations become more awkward. In practice, therefore, to determine the effective conductivity of an inhomogeneous system with a random component distribution, Eq. (8) is used most often.

2. Computer and Geometric Methods of Determining the Flow Threshold. Several methods are used to determine m_c. One of the main methods is a computer calculation, when m_c is determined by a computer Monte Carlo calculation [21-23]. To find it, there also exists the Domb and Sykes series method [24]. Sykes and Essam also suggested a method of calculating m_c, based on analyzing the coefficients of these series for various lattices. For several planar lattices these authors succeeded in obtaining exact results [25, 26]. In treating continuum problems the authors of [10, 12] showed by computer methods that, in the three-dimensional case, the flow threshold equals $m_c = 0.15 \pm 0.03$.

Another, less-well-known, method of finding m_c is the geometric method. The authors of [27] first determined m_c, starting from the assumption that to generate in a binary system with $m_M = m_i = 0.5$ a structure with mutually penetrating components (Fig. 3b) the maximum length of the cube edge ℓ_2 of an isolated inclusion (Fig. 3c) must equal $\ell_2 = 0.5$ L, whence one obtains $m_c = (\ell_2/L)^3 = 0.125$. In [28, 29] Dul'nev and Malarev determined by the geometric method the critical fluid concentrations (critical moisture contents) in humid disperse materi-

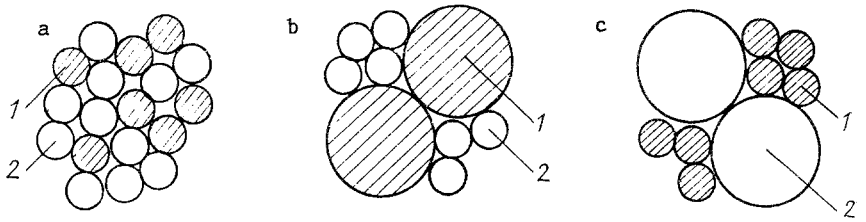

Fig. 4. Granular systems consisting of a conductor and insulator with particle diameters D and d (1, conductor; 2, insulator): a) particles of the same size z = d/D = 1; b) z < 1; c) z > 1.

als for various wetting angles. The results obtained are in good agreement with the results of flow theory. This subject is discussed in more detail in Sec. 4.

3. Polydisperse Materials. It was noted in [30, 31] that in a system consisting of large-scale conducting particles (diameter D) and small-scale isolating particles (diameter d), i.e., for z = d/D < 1, the decrease in conductivity in comparison with a system consisting of particles of the same size occurs due to the decrease in transverse cross-section area between conducting particles and the increase in curvature of current lines. It is further noted that if the isolating particles are larger (z > 1) they are "wedged in" between conducting grains at a lower depth (in comparison with particles of the same size), which enhances the minimum and effective transverse cross section of the conducting component particle chain and decreases the curvature of the current lines, thus reducing the medium resistance. In these studies it was experimentally found that the relation between conducting and insulating particle sizes affects the critical conducting concentration at which the system conductivity changes jumpwise. Consider conductivity processes through similar granular systems. The conduction analysis starts from a granular system (Fig. 4a) consisting of conducting and insulating particles of the same size (z = 1). In this system the conducting phase IFC can be formed both prior to compression, if the initial conducting concentration is $m_M^0 \approx 0.15$ (M is the conducting metal, i is the insulator, and p is the pore), and during the compression process. In this case the initial conducting concentration is in the interval

$$B \leqslant m_{\text{м}}^0 \leqslant 0.15, \tag{9}$$

where B is some boundary value of the conducting concentration, for which an IFC can still be formed. It can be shown that this occurs during compression up to the nonporous state ($m_p = 0$); therefore, $m_M^0 = (0.15/0.85)m_i^0$ and, consequently, $B = (3/17)m_i^0$. If $m_M^0 < B$, an IFC is not formed in the system at all for any value of finite porosity.

Based on the discussion above, we determine the critical value of conducting concentration x_c, which can be defined as the ratio of conducting volume V_M to the sum of conducting V_M and insulating V_i objects if an IFC is formed in the system:

$$x_c = \frac{V_{\text{м}}}{V_{\text{м}} + V_{\text{i}}} = \frac{V_{\text{м}}^0}{V_{\text{м}}^0 + V_{\text{i}}^0} = \frac{V_{\text{м}}^0}{V^0 - V_{\text{p}}^0} = \frac{m_{\text{м}}^0}{1 - m_{\text{p}}^0}, \tag{10}$$

where V^0 is the volume of the whole system prior to compression.

It is seen that the value of x_c depends on the initial porosity, and can vary from 0.15, if $m_M^0 = (3/17)m_i^0$, to 1 for $m_i^0 = 0$.

Consider now a system of large-scale conducting particles and small-scale insulating particles (Fig. 4b). It can be shown that the given case (z < 1) is similar to the preceding one, since in both cases the conducting particles are immersed in a quasihomogeneous medium, consisting of a mixture of insulating and porous space particles. In this case, the relation between sizes of insulating and conducting particles (i.e., the parameter z) does not affect the critical value of the conducting concentration x_c. The quantity x_c can be determined both from Eq. (10) and by means of the following expression:

$$x_c = \frac{0.15}{1 - m_{\text{p}}}, \tag{11}$$

where m_p implies the porosity value of the system, for which an IFC is formed during the compression process.

It was noted in [30, 31] that since the samples consisted of particles of different dispersivity, whose activities are not identical, then sample condensation also occurred with different intensity, and the samples prepared were characterized by different porosities; the sample porosity varied from 0.05 to 30%, depending on the technological regime. From (11) we obtain that for these m_p values x_c varies within the limits 0.15-0.21.

Consider the third case $z \gg 1$, i.e., the large-scale insulating particles are immersed in a quasihomogeneous medium, consisting of small-scale conducting particles and pores (Fig. 4c). The flow in this system starts when the volume of the conducting low-dispersion phase is 0.15 of the volume $V - V_i$:

$$m_м = 0.15(1 - m_i) = 0.15(m_м + m_p). \tag{12}$$

Expressing m_M in (12) in terms of m_p, with account of (11) we obtain $x_c = 3/17[m_p/(1 - m_p)]$. As in the case $z \leq 1$, it is seen that x_c depends on the porosity value at which an IFC is formed. At $m_p = 0.3$ we obtain $x_c = 0.08$. It was noted in [3] that for $z = 0.006$, x_c is of the order of 0.1. The relations given are valid for $z \gg 1$, while expressions for x_c are obtained for any $z > 1$.

A model was constructed in [32], reflecting the random character of the arrangement of isolated components in the volume of a two-component system with chaotic structure. In this case the transport process was not investigated over the whole volume of the chaotic system, but in a small portion of width h, commensurate with the mean distance between particle centers. It was shown in that study that the equation for the mean statistical distance $\langle \ell \rangle$ between centers of conducting particles with characteristic particle size D is, depending on the concentration,

$$\langle l \rangle = k_f D m_м^{-1/3}, \tag{13}$$

where for spherical particles $k_f = 0.806$.

The maximum diameter of insulating particle d_0 can be determined by placing it in the segment between conducting particles without destroying the structure of their arrangement (Fig. 5). The following expression is valid in this case:

$$\frac{D + d_0}{2} = \frac{\sqrt{3}}{2} \langle l \rangle, \tag{14}$$

from which, using (13), we obtain

$$d_0 = D(\sqrt{3} k_f m_м^{-1/3} - 1). \tag{15}$$

If instead of particles of diameter d_0 one now places in the elementary unit cell an insulating particle with diameter $d > d_0$, the volume of the conducting phase V_M^* in the unit cell is diminished from the initial V_M by the value $\pi/6(d^3 - d_0^3)m_M$, i.e.,

$$V_м^* = V_м - \frac{\pi}{6} m_м (d^3 - d_0^3). \tag{16}$$

We transform (16) with account of the fact that $V_i = (\pi/6)d^3$:

$$V_м^* = V_м - m_м V_i \left(1 - \left(\frac{d_0}{d}\right)^3\right), \tag{17}$$

or

$$m_м^* = m_м \left(1 - m_i \left(1 - \left(\frac{d_0}{d}\right)^3\right)\right). \tag{18}$$

We assume that an IFC ($m_M = 0.15$) has existed in the system prior to mixing. As a result of mixing the conducting low-dispersion phase with the high-dispersion phase of the insulator we obtain

$$m_м^* = 0.15 \left(1 - m_i \left(1 - \left(\frac{d_0}{d}\right)^3\right)\right). \tag{19}$$

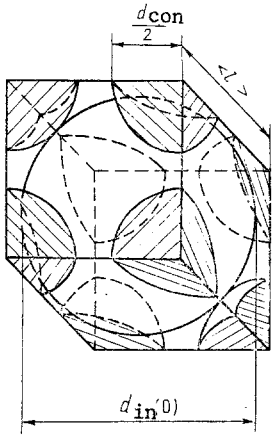

Fig. 5. Definition of the diameter d_0.

With account of (15), Eq. (19) acquires the form

$$m_{\text{м}}^{*} = 0.15\left(1 - m_{\text{i}}\left(1 - \frac{4.307}{z^3}\right)\right). \tag{20}$$

It is seen that (20) transforms to (12) for $z \to \infty$, and the m_M^* value for z = 1.627 (i.e., of the order of 1) equals $m_c = 0.15$, and starts decreasing with increasing z.

Equation (20) can be written somewhat differently, using the fact that $m_i = 1 - m_M^* - m_p$:

$$m_{\text{м}}^{*} = \frac{0.15\left(1 - (1 - m_{\text{p}})\left(1 - \frac{4.307}{z^3}\right)\right)}{0.85 + \frac{0.646}{z^3}}. \tag{21}$$

Starting from this point, the equation for x_c is:

$$x_{\text{c}} = \frac{0.15\left(1 - (1 - m_{\text{p}})\left(1 - \frac{4.307}{z^3}\right)\right)}{(1 - m_{\text{p}})\left(0.85 + \frac{0.646}{z^3}\right)}. \tag{22}$$

The authors of [30, 31] have derived the following expressions for determining x_c:

$$\begin{aligned} x_{\text{c}} &= 0.32\,\text{arctg}\,(0.55z^{-0.1}), \\ x_{\text{c}} &= 0.16 + 0.026\,\lg(1/z). \end{aligned} \tag{23}$$

These equations are approximate, are valid in a restricted range of variation in z, they do not satisfy the limiting transitions, and do not reflect the dependence of x_c on the system porosity. Therefore, for practical calculations it is recommended to use Eqs. (10) and (22).

Thus, in this section we have analyzed the effect of system dispersion on the critical concentration of the conducting phase x_c in the whole variation region of z, and have shown the dependence of this concentration on the system porosity.

4. Humid Materials. In investigating the thermal conductivity of humid porous materials one often uses modeling methods taking into account both the material structure and the occurrence of heat and mass transfer processes in it [33-37].

It was shown experimentally in [38] that the thermal conductivity of a humid material must depend substantially on the moisture distribution over the volume. The characteristic of surface wetting is usually the boundary wetting angle, formed on the boundary of a solid, fluid, or gas. The thermal conductivity of one and the same material with the same moisture content can differ by some factor, depending on the nature of moisture distribution in the material.

The authors of [28] suggested a model of humid, porous material, taking into account the effect of the nature of moisture distribution on transport processes. The model basically includes mutually penetrable components, containing a solid skeleton 1, a vapor-gas mixture 3, and moisture 2 (Fig. 6). At low moisture contents the fluid is distributed in the form of separated, isolated inclusions or isolated clusters (Fig. 6a), which increasingly grow at some critical value of solute moisture content $\omega = \omega'$ into one infinite cluster (Fig. 6b). With further increase in moisture content the fluid occupies a large fraction of porous space (Fig. 6c), while for value $\omega = \omega''$ the infinite cluster disappears from the mixture, and the vapor is now distributed in porous space in the form of isolated inclusions (Fig. 6d).

The effective thermal conductivity of this model was calculated on the basis of reducing these methods to an elementary unit cell with the use of flow theory (see Sec. 1). In this case, the analysis of heat and mass transfer processes in the three-component system was carried out by successively reducing it to a binary system [19]. For this one determines at the first phase the effective thermal conductivity of porous space, containing the fluid and the gas-vapor mixture; and at the second phase – the effective thermal conductivity of the whole material.

We represent the porous space, containing the fluid and the gas-vapor mixture, as a binary system of mutually penetrable components. For various values of moisture content the elementary unit cells of this system are represented in Fig. 3. It was noted above that for low moisture contents ($\omega < \omega'$) the fluid is concentrated in an isolated cluster (IC) in a cube of edge ℓ_2 (Fig. 3c), its concentration is $\omega = (\ell_2/L)^3$, and the ICs themselves are located at distance $\ell_3 = L - \ell_2$ from each other. For moisture contents $\omega \geq \omega'$ the ICs are combined by conducting bonds, whose transverse cross sections are $S_1 = \ell_1^2$ (Fig. 3a). In this case, according to flow theory, there exists a limiting value of the moisture content $\omega < \omega'$, for which $S_1 = 0$, while for $\omega = \omega'$ the first bridges are formed by a "jump," i.e., the isolated clusters are combined and transform to an infinite cluster (IFC). Further increase in ω leads to increasing the area of the transverse cross section ℓ_1^2 of the bridge until the ℓ_1 and ℓ_2 values are equal, and the heterogeneous system transforms to a structure with mutually penetrable components (Fig. 3b). With further increase in ω the transverse cross-section area ($L^2 - \ell_1^2$) of bridges of the gas-vapor component starts decreasing, and for fluid concentration $\omega = \omega''$ the IFC mixture of gas and vapor disappears. By purely geometric constructions it was shown in [28] that the values of ω' and $1 - \omega''$ are approximately equal to 0.16 in the middle of the porosity interval when the wetting angle ϑ equals 0. This conclusion is in good agreement with results of flow theory, starting from which the threshold flow is approximately equal to 0.15 for a two-component system in three-dimensional space.

The calculation of the effective thermal conductivity λ_{12} of an inhomogeneous binary system, consisting of a gas-vapor mixture 2 and a fluid 1 with thermal conductivities λ_2 and λ_1, can be carried out by Eq. (8), in which one must take:

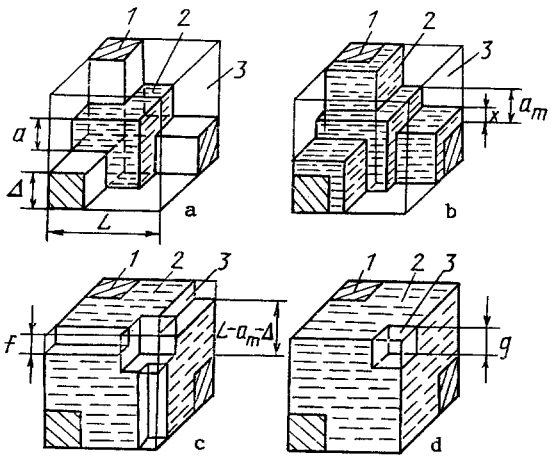

Fig. 6. Model of humid porous materials: a) $\omega < \omega'$; b) $\omega' \leq \omega \leq \omega^*$; c) $\omega^* \leq \omega \leq \omega''$; d) $\omega'' \leq \omega$ (1, solid phase; 2, fluid; 3, gas-vapor).

$$S_1 = \begin{cases} \left(\dfrac{\omega - \omega_c}{1 - \omega_c}\right)^{1.6}, & \omega \leqslant \omega^*, \\ \left(\dfrac{\omega_c - \omega}{\omega_c}\right)^{1.6}, & \omega > \omega^*; \end{cases} \tag{24}$$

$$\omega_c = \begin{cases} \omega', & \omega \leqslant \omega^*, \\ \omega'', & \omega > \omega^*; \end{cases} \tag{25}$$

$$\bar{l}_2 = \sqrt[3]{\omega_c}, \quad \nu = \lambda_2/\lambda_1,$$

where ω^* is the moisture content at which the fluid, along with the shell and the vapor-air mixture, form in pore space a structure with mutually penetrable components, in which case $x = a_m$ (Fig. 6b).

At the second phase of the calculation one determines by well-known equations [18, 19] the effective thermal conductivity λ of a humid material, which can be represented in the form of a structure with mutually penetrable components of a solid skeleton i = 3 and porous space i = 1, 2 (Fig. 3b). The effective thermal conductivity of a binary system with mutually penetrable components can be determined from the equation

$$\frac{\lambda}{\lambda_3} = c^2 + \nu(1-c)^2 + \frac{2\nu(1-c)c}{1-c+\nu c}, \quad \nu = \frac{\lambda_{12}}{\lambda_3}. \tag{26}$$

The parameter $c = \ell_1/L$ is determined by solving the cubic equation

$$m = 2c^3 - 3c^2 + 1, \tag{27}$$

where m is the material porosity.

Consider the effect of the wetting angle between a fluid and a solid shell on the threshold values of the moisture content in humid porous materials. Figure 7 shows one eighth of the elementary unit cell of a structure with mutually penetrable components for the critical values of moisture content $\omega = \omega'$ and $\omega = \omega''$ for the wetting angles $\vartheta = 0$, 45, and 90°. The value of the moisture content is related, by definition, to the voluems of the fluid V_f and the pore V_p by the dependence $\omega = V_f/V_p$. We find the ω' value for one of the cases, for example $\vartheta = 45°$. It follows from Fig. 7c that $V_f = 3V_1 + V_2$, $V_1 = 0.5\Delta(L-\Delta)^2$, $V_2 = (L-\Delta)^3/6$. Consequently, for the case considered the critical value of the moisture content ω' equals:

$$\omega' = \frac{\frac{1}{6}(L-\Delta)^3 + \frac{3}{2}(L-\Delta)^2\Delta}{(L-\Delta)^2(L+2\Delta)} = \frac{1}{6}\frac{1+8c}{1+2c}. \tag{28}$$

The values of ω' and ω'' can be obtained similarly for other wetting angles.

The dependence of ω' on the wetting angle ϑ can be approximated by a quadratic polynomial:

$$\omega' = a_0 + a_1\vartheta + a_2\vartheta^2. \tag{29}$$

Table 1 shows the values of a_0, a_1, and a_2 for various values of the direct porosity m_{dir}.

TABLE 1. Values of the Quantities a_0, a_1, and a_2 as a Function of Direct Porosity m_{dir}

m_{dir}	0,1	0,2	0,3	0,4	0,5	0,6
a_0	0,201	0,193	0,186	0,178	0,170	0,160
a_1	$5{,}48\cdot10^{-3}$	$5{,}68\cdot10^{-3}$	$5{,}40\cdot10^{-3}$	$5{,}13\cdot10^{-3}$	$4{,}87\cdot10^{-3}$	$4{,}56\cdot10^{-3}$
a_2	$1{,}36\cdot10^{-5}$	$6{,}17\cdot10^{-6}$	$8{,}89\cdot10^{-6}$	$1{,}14\cdot10^{-5}$	$1{,}38\cdot10^{-5}$	$1{,}68\cdot10^{-5}$

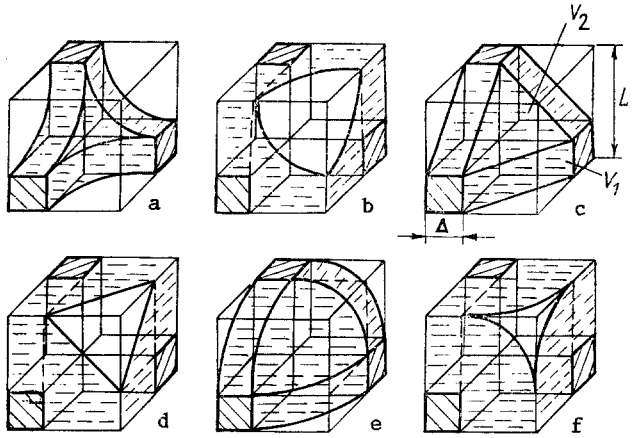

Fig. 7. The nature of fluid distribution in a shell-pore space structure for critical values of moisture content and various wetting angles: a) $\omega' = 0.16$, $\vartheta = 0°$; b) $\omega'' = 0.85$, $\vartheta = 0°$; c) $\omega' = 0.41$, $\vartheta = 45°$; d) $\omega'' = 0.96$, $\vartheta = 45°$; e) $\omega' = 0.75$, $\vartheta = 90°$; f) $\omega'' = 0.99$, $\vartheta = 90°$.

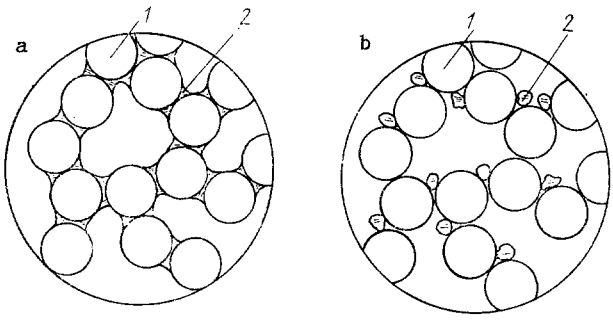

Fig. 8. Fluid distribution in the porous space of a grainy system (1, solid particles; 2, fluid disseminations); the fluid wets the particle surface: a) well; b) poorly.

If, following saturation by the fluid porous material up to moisture content ω', we start removing randomly portions of the fluid of the elementary unit cells, the fluid IFC disappears when only approximately 15% of all elementary unit cells remain humid. The concentration of the fluid component in a porous body equals in this case:

$$x_c = 0.15\omega' m_{\text{скв}}. \qquad (30)$$

The approach given of determining the concentration of the fluid component x_c can be used, for example, to find the allowed silicon concentration in porous baked carbide-silicon ovens. In passing an electric current through them, their temperature can exceed the melting temperature of silicon, as a result of which it flows into the porous space over the internal surface of the baked shell. Since the electric conductivity of silicon is substantially higher than the electric conductivity of the carbide-silicon shell, a silicon fluid phase IFC is generated in the system at a silicon concentration higher than x_c, and the oven resistance drops sharply, as a result of which it becomes disordered.

Based on analyzing the nature of the fluid distribution in porous space, the authors of [29] suggested a model and a method of calculating the effective thermal conductivity of humidity grainy materials. The effect has been shown of the nature of the fluid distribution in the structure of the grainy material on the value of the effective thermal conductivity. When the fluid wets the shell and forms aqueous bridges in the contact locations (Fig. 8a), the thermal conductivity of the whole system increases sharply due to the decrease in contact resistance between grains. If the fluid does not wet the particle surface, it is distributed by separate disseminations of noncontacting drops (Fig. 8b), as a result of which the effective thermal conductivity of the grainy system increases with increasing moisture content substantially more slowly, since the dry shell of grains seems to have an insulating effect.

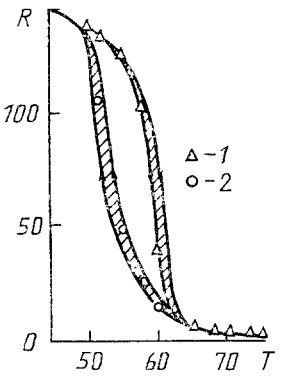

Fig. 9. Temperature dependence of the electric resistance in VO_2: 1) experimental values, measured for increasing temperature; 2) same for decreasing temperature [39]. Solid lines) calculated values for $0.12 \leq m_c \leq 0.18$. R, Ω; T, °C.

The method of calculating the effective thermal conductivity of humid grainy systems is based on the assumption that a shell of particles can be isolated in the system and be found in contact locations of moist particles (when the fluid wets the grain surfaces). The remaining portion of porous space, which can in turn be either a single-phase or two-phase system, can be considered in the set with a separate shell as a structure with mutually penetrable components. The effective thermal conductivity of this model was calculated by using a method of reduction to an averaged element of the grainy system with account of wetting by fluid particles.

5. Conductivity for Structural Phase Transitions. Materials are known whose conductivity varies due to the structural phase transition in materials [39, 40]. For example, a substantial conductivity variation in a relatively narrow temperature interval occurs in vanadium oxide VO_2 (a metal-semiconductor phase transition), in titanium-barium based ceramic $BaTiO_3$ (a ferroelectric-paraelectric transition), and in partially crystalline polymers (for example, polyethylenes, polypropylenes) [42]. The structural phase transition occurs in the relatively narrow temperature range $\Delta T = T_i - T_f$, where T_i and T_f are the initial and final phase transition temperatures. At temperatures $T < T_i$ there exists a structurally uniform phase, characterized by the conductivity Λ_1 (electric conductivity σ_1, thermal conductivity λ_1) and temperature coefficient α_1. Above $T > T_f$ a different structurally uniform phase is generated with parameters Λ_2 and α_2. According to the theory of heterogeneous transformations, the generation of the new phase in the original matrix occurs due to nucleus formation and the growth of a new phase [41]. The conductivity of this type of structures can be described by the dependences (8), taking into account percolation effects. In this case, it is necessary to relate the concentration m_i of phase i with temperature $m_i = m_i(T)$. Combining these equations makes it possible to obtain the temperature dependence $\Lambda = \Lambda(\Lambda_i, T)$ of the conductivity under conditions of a structural phase transition. It can be shown that the process of nucleus formation is related to the existence of heterophase fluctuations, and their concentration is proportional to the internal energy reserve of the solid. The temperature dependence of the new phase nucleus concentration is then acquired by the similar temperature dependence of the specific heat. Following nucleus formation, they grow due to fluctuations generated near the separation between the two phases, i.e., near the nucleus, and the latter process is characterized by the entropy value of the activation process [43].

We denote the bulk heat capacity by C_V, the entropy variation during phase transition by ΔS, and the bulk concentration by m_2. Normalizing over the temperature region $(T_f - T_i)$, the authors of [43] derive the equation

$$m_2 = \frac{c_v - c_{vi}}{c_{vf} - c_{vi}} \frac{\Delta S - \Delta S_i}{\Delta S_f - \Delta S_i}. \quad (31)$$

It is assumed in [43] that the relation between C_V and temperature is determined by the Einstein–Nernst–Lindeman equation, and that the quantity ΔS is calculated from data on the transformation heat ΔH during phase transition:

$$\Delta H = T\Delta S. \quad (32)$$

Equations (8), (31), and (32) make it possible to obtain the required dependence $\Lambda = \Lambda(T)$. For thermoresistors of vanadium oxide, operating at the metal-semiconductor phase transition, temperature dependence of electric resistivity $R = \Lambda^{-1}$ possesses, as seen from Fig. 9, a temperature hysteresis: at the same temperatures the bulk concentrations m_1' and

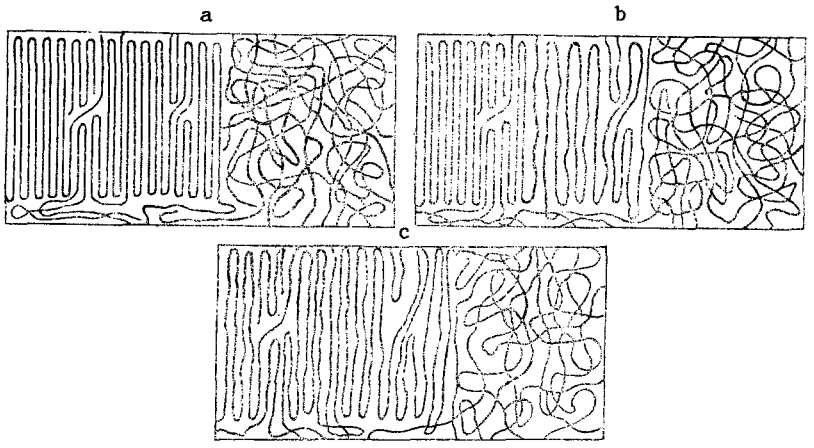

Fig. 10. Model of a partially crystalline polymer: a) $T = T_g$; b) $T_g < T < T_m$; c) $T \geq T_m$.

m_2'' of the metallic phase are different for increasing and decreasing temperature [39]. The occurrence of hysteresis follows formally from the structure of dependence (31). We write it down for the direct and inverse branches of the curve $R = R(T)$, keeping in mind that for these branches the locations of the initial T_i and final T_f temperature values and the quantities corresponding to them C_v and ΔS change:

$$m_2' = \frac{c_v - c_{vi}}{c_{vf} - c_{vi}} \frac{\Delta S - \Delta S_i}{\Delta S_f - \Delta S_i}, \quad m_2'' = \frac{c_v - c_{vf}}{c_{vi} - c_{vf}} \frac{\Delta S - \Delta S_f}{\Delta S_i - \Delta S_f}. \tag{33}$$

It follows from (33) that $m_2' \neq m_2''$, and the dependence (33) is not invariant to the direction of the process, i.e., hysteresis is possible for structural phase transitions. The latter can also be generated by other processes, such as the percolation effect. Since $m_c = 0.15 \pm 0.03 = 0.12\text{-}0.18$, smearing of the direct and inverse branches is possible and they can overlap, so that hysteresis is not manifested directly, as illustrated by the temperature dependence $R = R(T)$ for a semiconducting ceramic on a titanium-barium base in the ferroelectric-paraelectric phase transition region [43].

Methods of calculating the thermal conductivity of partially crystalline polymers in the temperature interval from glass formation T_g to melting T_m were considered in [42]. Depending on the features of the polymerization process, the polymers obtained differ in the method of crystalline structure formation: the shape and mutual location of macromolecule segments form a crystalline lattice, while the chain branching and the regularity of its structure exclude this possibility as well as the intermediate case (partially crystalline polymers). Polymers of the latter type are commonly characterized by the extent of crystallization α_g, equal to the ratio of the number of crystallizing and noncrystallizing modifications at the glass formation temperature (the original extent of crystallization). At temperatures exceeding T_g the crystalline portions melt, but the locations of macromolecular chains in them do not become totally disordered – the chain portions basically retain parallel stacking (Fig. 10). For $T_g < T$, there are crystalline formations and portions not possessing long-range order, but differing in density and nature of packing of macromolecular segments from the noncrystalline modification – the quasiamorphic modification. Starting from glass formation, with increasing temperature all crystallizing modifications transform from crystalline to the quasiamorphic state, and the composite structure also contains other formations. Thus, a partially crystalline polymer contains amorphous, quasiamorphous, and crystalline components. Above the glass formation temperature we have melting of the crystalline portions; for high extent of crystallization (95%) the crystalline portions fuse and form the system shell; near the melting temperature crystalline formations exist in the form of closed inclusions in the matrix, consisting of amorphous and quasiamorphous modifications. During crystallization from the melt we have the same, but in reverse order: the appearance of isolated crystalline inclusions, generation of contacts between them, their growth, and, finally, formation of a continuous shell of crystalline portions. This structure is adequately treated in Sec. 1 of the model, whose thermal conductivity can be described by Eqs. (8), where the conducting component has thermal conductivity λ_c (crystalline portion), a bulk concentration $m = \alpha^V$, equal to the bulk extent of crystallization, and the nonconducting is λ_a (amorphous and quasiamorphous portions).

The polymer as a whole is a conducting matrix with nonconducting inclusions. The bulk fraction of the latter m_f increases during the process of phase transition, melting of the crystalline portions, and can be calculated in each temperature interval ΔT from the temperature dependence of the decrystallization rate [42]

$$m_f = \left| \frac{\overline{\partial \alpha}}{\partial T} \right|_{\Delta T_i} \Delta T_i.$$

For $m_f < 0.15$, Eq. (8) acquires the form

$$\lambda = \lambda_M \left(\frac{m_f^{1/3}}{1 - (1 - \nu) m_f^{1/3}} + (1 - m_f)^{2/3} \right). \tag{34}$$

For $m_f > 0.5$, the thermal conductivity is calculated by Eq. (8), where $m = 1 - m_f$.

Thus, the calculation of λ of a partially crystalline polymer is carried out in two steps: first one calculates the thermal conductivity λ_M of the matrix consisting of crystalline and amorphous portions; second, one evaluates the whole polymer, i.e., the system consisting of the matrix and of portions undergoing a phase transition.

The λ_c and λ_a values required for the calculation can be evaluated in the presence of experimental data on the thermal conductivity of two polymer samples with different original extents of crystallization. In [42], for example, these dependences $\lambda = \lambda(T, \alpha_g)$ are evaluated for polyethylene at low and high density.

By this method one can calculate the thermal conductivity of a partially crystalline polymer in the temperature interval from glass formation to melting. In this case, the deviation between calculated thermal conductivity values and experimental values is commensurate with the experimental error, i.e., 8-10%.

6. Mechanical Properties; Penetrability. The geometric IC and IFC forms, flow theory, and the generalized conductivity were used by V. V. Novikov to investigate mechanical properties of inhomogeneous media. Particularly investigated were the thermal expansion coefficient (TEC) of a polymer matrix, carbon fiber [44]; calculations have shown that the TEC of a fibrous structure is quite sensitive to variations in the elastic properties of the fiber; and variation of the latter by 30-50% leads to TEC variations of the composite by two to three times.

The nature of the problem required transformation from vector to tensor analysis problems; in other words, the dependence obtained for the conductivity of inhomogeneous media cannot be transferred to the elastic properties. It has been established that the analogy between elasticity and conductivity of a microscopically inhomogeneous material can be carried out only if one neglects the elastic interaction between components. This leads to a substantial error in determining the elastic properties of inhomogeneous materials.

In particular, during IFC formation and for $m_1 = m_c = 0.15$ no macroscopic rigidity can be generated in the system, this threshold equals $m_c^* = 0.3$-0.43, and the elastic moduli (the uniform compression modulus K and the shear modulus) are determined in the form $K \sim \mu^P \sim (m_1 - m_c^*)^f$, $f = 3.6 \pm 0.6$.

The elastic moduli K, μ^P, and the TEC α were determined in [45] for percolation models, and their unusual behavior in comparison with conductivity was shown. The elastic properties of powder materials, porous metals, and pseudoalloys were investigated in [46]. Similar structural models and calculation methods were described, with the analytic and experimental data found in satisfactory agreement.

The percolation models also made it possible to describe the penetrability of porous media. The definition of the penetrability k follows from Darcy's law, relating the fluid flow **V** with viscosity and the pressure gradient grad P: $\mathbf{V} = -(k/\mu)\,\mathrm{grad}\,P$. The structure of this equation recalls the Fourier and Ohm laws, making it possible to use the thermoelectric analogy, while the description of the structure is carried out with account of IC and IFC formation; then the value k of porous materials can be obtained on the basis of dependences (8), since $k = \Lambda$ can be assumed to be a generalized conductivity coefficient. Assuming the penetrability of the continuous solid shell to vanish, i.e., $K_2 = 0$, and the pore penetrability to be $-k_1$, $k = k_1 c^2$. Further analysis of this process is carried out in [47] and makes it possible to calculate the penetrability of solid and grainy porous systems with account of IFC formation, its winding, and other parameters.

NOTATION

m_M, m_i, bulk concentrations of the conducting and insulating phases; m_c, threshold concentration value; L, size of the element shown; d, D, particle diameters of the insulator and conductor, in m; V_M^0, V_i^0, V_p^0, V_M, V_i, V_p, volumes of the conducting, insulating, and porous phases up to and following compression, in m^3; x_c, critical concentration, referring to the sum of conducting and insulating volumes; k_f, particle shape coefficient; $\langle \ell \rangle$, statistical mean distance between centers of conducting particles, in m; ω, moisture content; ω', ω'', critical values of the moisture content; ϑ, wetting angle, deg; λ, thermal conductivity of the material, W/(m·K); T, temperature, K; ΔH, transformation heat during phase transition, J/mole/ C_v, bulk specific heat capacity, J/(kg·K); α_g, extent of polymer crystallization; P, pressure, Pa; k, material penetrability, m^2.

LITERATURE CITED

1. S. R. Broadbent and J. M. Hammersley, Proc. Cambridge Phil. Soc., 53, 629-645 (1957).
2. S. Kirkpatrick, Rev. Mod. Phys., 45, No. 4, 575-610 (1973).
3. B. I. Shklovskii and A. L. Éfros, Usp. Fiz. Nauk, 117, No. 3, 401-434 (1975).
4. B. I. Shklovskii and A. L. Éfros, Electronic Properties of Alloyed Semiconductors [in Russian], Moscow (1979).
5. S. P. Obukhov, in: Proc. 4th All-Union Conf. Mathematical Methods in the Study of Polymers and Biopolymers [in Russian], Pushchino (1985).
6. A. M. El'yashevich, in: Proc. Conf. Problems of Polymer Theory in the Solid Phase [in Russian], Chernogolovka (1985).
7. A. L. Éfros, Physics and Geometry of Disorder [in Russian], Leningrad (1981).
8. Kh. Kesten, Theory of Wetting for Mathematicians [Russian translation], Moscow (1986).
9. A. S. Skal and B. I. Shklovskii, Fiz. Tekh. Poluprovod., 8, No. 8, 1586-1592 (1974).
10. V. K. Shante and S. Kirkpatrick, Adv. Phys., 20, No. 85, 325-357 (1971).
11. I. Webman, J. Jortner, and M. Cohen, Phys. Rev., B11, No. 8, 2885-2903 (1975).
12. I. Webman, J. Jortner, and M. Cohen, Phys. Rev., B13, No. 2, 713-727 (1976).
13. D. A. G. Von Bruggemann, Ann. Phys., 24, No. 7, 636-652 (1935).
14. E. I. Kondorskii, Izv. Akad. Nauk SSSR, Ser. Geogr. Geofiz., 14, No. 4, 57-68 (1950).
15. Yu. A. Buevich, Prikl. Mekh. Tekh. Fiz., No. 4, 57-68 (1973).
16. A. F. Chudnovskii, Thermophysical Characteristics of Disperse Materials [in Russian], Moscow (1962).
17. G. N. Dul'nev and V. V. Novikov, Inzh.-Fiz. Zh., 36, No. 5, 901-910 (1979).
18. G. N. Dul'nev, Transport Coefficients in Inhomogeneous Media [in Russian], Leningrad (1979).
19. G. N. Dul'nev and Yu. P. Zarichnyak, Thermal Conductivity of Mixtures and Composite Materials [in Russian], Leningrad (1974).
20. G. N. Dul'nev and V. V. Novikov, Inzh. Fiz. Zh., 45, No. 3, 443-451 (1983).
21. H. L. Frisch, J. M. Hammersley, and D. J. A. Welsh, Phys. Rev., 126, 949-982 (1962).
22. V. A. Vyssotsky, S. B. Gordan, H. L. Frisch, and J. M. Hammersley, Phys. Rev., 123, 1566-1580 (1961).
23. P. Dean, Proc. Camb. Phil. Soc., 59, 397-415 (1963).
24. G. Domb and M. F. Sykes, Phys. Rev., 122, 77-96 (1960).
25. M. F. Sykes and J. M. Essam, Phys. Rev. Lett., No. 10, 23-27 (1963).
26. M. F. Sykes and J. M. Essam, J. Math. Phys., No. 5, 1117-1126 (1964).
27. V. A. Osipova and Kh. A. Kyaar, Atomnaya Energiya, 32, No. 2, 31-40 (1972).
28. G. N. Dul'nev, D. P. Volkov, and V. I. Malarev, Inzh. Fiz. Zh., 56, No. 2, 291-291 (1989).
29. G. N. Dul'nev and V. I. Malarev, Inzh. Fiz. Zh., 56, No. 1, 141-142 (1989).
30. Yu. P. Zarichnyak, S. S. Ordan'yan, A. N. Sokolov, and E. K. Stepanenko, Poroshkovaya Metallurgiya, No. 7, 64-71 (1986).
31. Yu. P. Zarichnyak, S. S. Ordan'yan, A. N. Sokolov, and E. K. Stepanenko, Poroshkovaya Metallurgiya, No. 6, 97-101 (1986).
32. Yu. P. Zarichnyak and V. V. Novikov, Inzh. Fiz. Zh., 32, No. 4, 648-655 (1978).
33. O. Krisher, Scientific Foundation of Drying Technology [Russian translation], Moscow (1961).
34. G. N. Dul'nev, Yu. P. Zarichnyak, and B. L. Muratova, Inzh. Fiz. Zh., 31, No. 2, 278-283 (1976).
35. V. G. Petrov-Denisov and A. A. Maslennikov, Processes of Heat and Moisture Exchange in Industrial Insulation [in Russian], Moscow (1983).

36. L. P. Volkov, G. N. Dul'nev, V. L. Muratova, and A. B. Utkin, Inzh. Fiz. Zh., 50, No. 6, 939-946 (1986).
37. A. V. Lykov, Handbook on Heat and Mass Transfer [in Russian], Moscow (1978).
38. A. F. Begunkova, G. N. Dul'nev, V. L. Muratova, et al., Inzh.-Fiz. Zh., 31, No. 6, 974-980 (1976).
39. I. T. Sheftel', Thermoresistors [in Russian], Moscow (1972).
40. V. N. Novikov, B. A. Tallergin, E. I. Gindin, and V. G. Prokhvatilov, Fiz. Tverd. Tela (Leningrad), 12, 2565-2583 (1970).
41. S. A. Medvedev, Introduction to Technology of Semiconducting Materials [in Russian], Moscow (1970).
42. T. L. Shimchuk, A. N. Piven', and Yu. F. Voikov, Inzh.-Fiz. Zh., 45, No. 3, 443-452 (1983).
43. G. N. Dul'nev, I. K. Meshkovskii, V. V. Novikov, and I. A. Sokolov, Inzh.-Fiz. Zh., 37, No. 2, 229-235 (1979).
44. V. V. Novikov, Inzh.-Fiz. Zh., 47, No. 4, 617-624 (1983).
45. V. V. Novikov, Prikl. Mekh. Tekh. Fiz., No. 4, 146-153 (1985).
46. V. V. Novikov, Fiz. Met. Metalloved., 58, No. 3, 598-604 (1984).
47. D. P. Volkov, Inzh.-Fiz. Zh., 41, No. 3, 421-427 (1981).